European Journal of Pharmacology 866 (2020) 172810

Contents lists available at ScienceDirect

European Journal of Pharmacology

journal homepage: www.elsevier.com/locate/ejphar

Full length article

Empagliflozin restores lowered exercise endurance capacity via the activation of skeletal muscle fatty acid oxidation in a murine model of heart failure

Hideo Nambu[a,1], Shingo Takada[a,b,*,1], Arata Fukushima[a], Junichi Matsumoto[a], Naoya Kakutani[a,c], Satoshi Maekawa[a], Ryosuke Shirakawa[a], Ippei Nakano[a], Takaaki Furihata[a], Takashi Katayama[a], Katsuma Yamanashi[a], Yoshikuni Obata[a], Akimichi Saito[d], Takashi Yokota[a], Shintaro Kinugawa[a]

[a] Department of Cardiovascular Medicine, Faculty of Medicine and Graduate School of Medicine, Hokkaido University, Sapporo, Japan
[b] Department of Lifelong Sport, School of Sports Education, Hokusho University, Ebetsu, Japan
[c] Research Fellow of the Japan Society for the Promotion of Science, Japan
[d] Institute of Preventive Medical Sciences, Health Sciences University of Hokkaido, Sapporo, Japan

ARTICLE INFO

Keywords:
Myocardial infarction
Exercise intolerance
Mitochondria
SGLT2 inhibitor
Ketone body
Muscle strength

ABSTRACT

Decreased exercise capacity, which is an independent predictor of the poor prognosis of patients with heart failure (HF), is attributed to markedly impaired skeletal muscle mitochondrial function and fatty acid oxidation. Previous studies reported that the administration of an inhibitor of sodium-glucose cotransporter 2 (SGLT2) increases ketone body production and fat utilization in type 2 diabetic mice. In this study, we investigated the effects of SGLT2 inhibitor administration on exercise endurance and skeletal muscle mitochondrial function with fatty acid oxidation in a murine model of HF after the induction of myocardial infarction (MI). Two weeks post-MI, HF mice were divided into 2 groups, i.e., with or without treatment with the SGLT2 inhibitor empagliflozin (Empa, 300 mg/kg of food). Consistent with previous studies, urinary glucose and blood beta-hydroxybutyrate levels were increased in the HF + Empa mice compared with the sham and HF mice 4 weeks after the start of Empa administration. Exercise endurance capacity was limited in the HF mice but was ameliorated in the HF + Empa mice, without any effects on cardiac function, food intake, spontaneous physical activity, skeletal muscle strength, and skeletal muscle weight. Mitochondrial oxidative phosphorylation capacity with fatty acid substrates was reduced in the skeletal muscle of HF mice, and this decrease was ameliorated in the HF + Empa mice. Our results demonstrate that SGLT2 inhibitors may be novel therapeutics against reduced exercise endurance capacity in HF, by improving mitochondrial fatty acid oxidation in skeletal muscle.

1. Introduction

The effects of empagliflozin (Empa), an inhibitor of sodium-glucose cotransporter 2 (SGLT2) on cardiovascular outcomes were investigated in patients with type 2 diabetes with high cardiovascular risk in the EMPA-REG OUTCOME trial (Zinman et al., 2015). The results of the trial showed that Empa administration leads to a significantly lower risk of death from cardiovascular causes and hospitalization for heart failure (HF). Changes in energy metabolism and shifts of energy substrates in the heart have been considered to be associated with the beneficial effects of SGLT2 inhibitors on cardiovascular outcome (Lytvyn et al., 2017). However, the underlying mechanism has not yet been elucidated.

Reduced exercise capacity, which is an independent predictor of the poor prognosis of patients with HF (Goda et al., 2011), is partly attributed to impaired skeletal muscle energy metabolism, including mitochondrial dysfunction (Kinugawa et al., 2015; Okita et al., 2013). We established a murine model of HF after myocardial infarction (MI), showing reduced fatty acid oxidation in the skeletal muscle, which is a clinical feature of patients with HF (Matsumoto et al., 2018; Takada

* Corresponding author. Department of Cardiovascular Medicine, Faculty of Medicine and Graduate School of Medicine, Hokkaido University, Kita-15, Nishi-7, Kita-ku, Sapporo, 060-8638, Japan.
E-mail address: s-takada@hotmail.co.jp (S. Takada).
[1] These authors contributed equally to this work.

https://doi.org/10.1016/j.ejphar.2019.172810
Received 13 October 2019; Received in revised form 14 November 2019; Accepted 14 November 2019
Available online 15 November 2019

et al., 2016; Tsuda et al., 2018). We also reported that the indirect enhancement of fatty acid oxidation through dipeptidyl peptidase-4 (DPP-4) inhibition in this HF model prevented skeletal muscle mitochondrial dysfunction, leading to the protection of lowered exercise capacity (Matsumoto et al., 2018; Takada et al., 2016). Exercise therapy is the most established approach to treat exercise intolerance in HF. However, exercise therapy is often impractical or inefficient for individuals who suffer from severe symptoms of HF. On the other hand, several pharmacological and surgical therapies have been known to effectively improve the reduced exercise capacity in patients with HF (Abbate et al., 2015; Kosmala et al., 2016). Most of these therapies have improved exercise intolerance through improvements in hemodynamics or cardiac remodeling. However, some patients with HF are resistant to these therapies and effective therapies for exercise intolerance are not yet enough. Thus, the development of a new therapeutic strategy for HF that targets skeletal muscle abnormalities is a crucial issue.

Therefore, we conducted the present study to determine the therapeutic effects of an SGLT2 inhibitor on the reduced exercise endurance capacity and skeletal muscle mitochondrial dysfunction, specifically, impaired fatty acid oxidation, in a murine model of HF.

2. Materials and methods

All procedures and animal care were approved by our institutional animal research committee (#16-0115) and conformed to the Animal Care Guidelines for the Care and Use of Laboratory Animals at Hokkaido University Graduate School of Medicine. Procedures and care were also in accordance with relevant national and international guidelines and the Guide for the Care and Use of Laboratory Animals published by the U.S. National Institutes of Health.

2.1. Murine model of HF after MI

Male C57BL/6J mice (10–12-weeks old, body weight [BW] 23–25 g, CLEA Japan, Tokyo) were bred in a pathogen-free environment and housed in an animal room under controlled conditions on a 12-hr light/dark cycle maintained at 23–25 °C. Normal diet and water were provided *ad libitum*. The MI was created by ligating the left coronary artery, as described previously (Fukushima et al., 2014, 2016a; Maekawa et al., 2019; Matsumoto et al., 2018; Sobirin et al., 2012; Takada et al., 2016). A sham operation without ligation of the coronary artery was also performed in some mice. For either operation, the mouse was anesthetized via intraperitoneal (i.p.) administration of the following mixture of drugs: 0.3 mg/kg BW of medetomidine (Dorbene®, Kyoritsuseiyaku Co., Tokyo), 4 mg/kg BW of midazolam (Dormicum®, Astellas Pharma, Tokyo), and 5 mg/kg BW of butorphanol (Vetorphale®, Meiji Seika Kaisha, Tokyo). The adequacy of the anesthesia was monitored based on the disappearance of the pedal withdrawal reflex.

Two weeks after the sham (n = 11) or MI (n = 32) surgery, HF mice were divided into 2 groups according to treatment with or without the SGLT2 inhibitor empagliflozin (Empa, 300 mg/kg of food, provided by Boehringer Ingelheim, Ingelheim, Germany) for 4 weeks. The dose of Empa was determined on the basis of previous pharmacodynamics studies (Lin et al., 2014; Vallon et al., 2014). In the study examining phamacokinetica and pharmacodynamics of SGLT-2 inhibitors, half-life of the drug is very short in mice compared to in human (Tahara et al., 2016). Therefore, to preserve the effective blood concentration of the drug, the use of high dose of empagliflozin in the experiments of mice is reasonable. Therefore, we thought that this amount may be appropriate when examining the effect of empagliflozin in mice experiments to maintain the effective blood concentration of the drug. We used the following three groups of mice: (1) sham (n = 11), (2) sham + Empa supplemented in the diet (n = 4), (3) HF (n = 9), and (4) HF + Empa (n = 10). These assignment procedures were performed using numeric codes to identity the animals (Fig. 1).

After 4 weeks of treatment/nontreatment, the mice were analyzed by echocardiography, a glucose test using the tail vein, and an exercise endurance test. The mice were then killed, and skeletal muscles were excised. Biochemical measurements, analysis of mitochondrial respiration, histological analysis, and immunoblotting were also performed.

2.2. Biochemical measurements

Urinary and blood samples were drawn from the tail vein. Glucose levels were determined using a glucometer (Glutest Ace R; Sanwa Kagaku Kenkyusho, Nagoya, Japan). Serum insulin levels were measured using an ELISA kit (Morinaga Institute of Biochemical Science, Yokohama, Japan). Total free fatty acids (FFAs) was measured using the NEFA C-test (Wako Pure Chemical Industries, Osaka, Japan). Serum beta-hydroxybutyrate (β-OHB) levels were measured using the beta-HB Assay Kit (Abcam, Cambridge, UK).

2.3. Exercise endurance, strength, and spontaneous physical activity

Exercise endurance was evaluated by measuring how long the mouse was able to hang upside down from a wire screen, as previously described (Rebo et al., 2016). Briefly, the mouse was placed on a 1-cm mesh screen made of 1-mm wires set 30 cm over soft bedding. The screen was then inverted, and the time until the mouse fell from the screen was measured. Two to three trials were conducted for each mouse with a ≥ 5-min rest between trials. The maximum hang time per weight of the mouse was calculated, in which longer times per weight for a given mouse was considered as the best performance, as described previously (Rebo et al., 2016).

Forelimb grip strength was evaluated using a triangular pull bar attached to a grip-strength meter (Columbus Instruments, Columbus, OH, USA). Each mouse was subjected to 5 consecutive tests to obtain the peak value, as previously described (Camporez et al., 2016).

Spontaneous physical activity was measured using an animal movement analysis system (ACTIMO System; Shintechno, Fukuoka, Japan), as described previously (Matsumoto et al., 2018; Takada et al., 2016).

2.4. Tissue preparation and histology

The heart, lung, epididymal white adipose tissue (EWAT), and unilateral hindlimb skeletal muscle were excised and weighed. The gastrocnemius muscle was used in all experiments. For histological analysis, the gastrocnemius muscle was fixed in 6% formaldehyde and stained with hematoxylin-eosin, as described previously (Takada et al., 2016).

2.5. Echocardiographic measurements

Echocardiographic measurements were performed after the 4 weeks of treatment, under light anesthesia with tribromoethanol/amylene hydrate (Avertin; 200 mg/kg BW, i.p.), which is reported to have a short duration of action and modest cardiodepressive effects, and to enable spontaneous respiration (Fukushima et al., 2014, 2016b; Matsumoto et al., 2018; Sobirin et al., 2012; Takaaki Furihata et al., 2016). A commercially available echocardiography system (Aplio™300, Toshiba Medical Systems, Odawara, Japan) was used with a dynamically focused 12-MHz linear array transducer and a depth setting of 2.0 cm. Two-dimensional parasternal short-axis views were obtained at the levels of the papillary muscles. In general, the best views were obtained with the transducer lightly applied to the mid-upper left anterior chest wall. The transducer was then gently moved in a cephalad or caudad direction and angulated until desirable images were obtained. Two-dimensional targeted M-mode tracings were recorded at a paper speed of 50 mm/s.

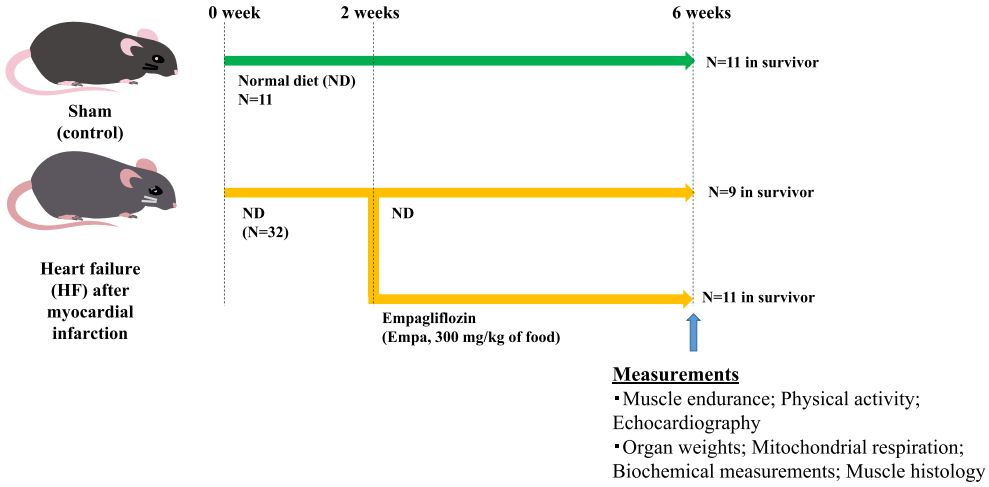

Fig. 1. Experimental protocol.

2.6. Preparation of permeabilized fibers

After careful dissection of the muscle tissue, the fiber bundles were permeabilized by gentle agitation for 30 min in an ice-cold relaxing BIOPS solution (in mmol/l: CaK_2EGTA [2.77], K_2EGTA [7.23], Na_2ATP [5.77], $MgCl_2 \cdot 6H_2O$ [6.56], taurine [20], Na_2phosphocreatine [15], imidazole [20], dithiothreitol [0.5], MES hydrate [50], pH 7.1) with saponin (50 μg/ml), as described (Takada et al., 2016). After permeabilization, fibers were rinsed twice by agitation for 10 min in the ice-cold respiration medium MiR05 (in mmol/L: sucrose [110], K-lactobionate [60], EGTA [0.5], $MgCl_2$ [3], taurine [20], KH_2PO_4 [10], 4-(2-hydroxyethyl)-piperazineethanesulfonic acid [20], 1% bovine serum albumin, pH 7.1), as described previously (Matsumoto et al., 2018; Takada et al., 2016).

2.7. Measurement of mitochondrial oxidative phosphorylation (OXPHOS) capacity with fatty-acid substrates in permeabilized fibers

Mitochondrial respiratory capacity with fatty-acid substrates in permeabilized skeletal muscle fibers at 37 ˚C was measured using a high-resolution respirometer (Oxygraph-2k, Oroboros Instruments, Innsbruck, Austria), as described previously (Takada et al., 2016). All respiratory measurements were carried out in duplicate after hyperoxygenation to avoid any potential O_2 limitations. Datlab software (Oroboros Instruments) was used for the data acquisition and analysis.

The following 2 protocols were used for the fatty-acid substrates measure OSPHOS capacity. A medium-chain fatty acid (octanoyl-l-carnitine) was used as the fatty-acid substrate. Because an excess of fatty acid may have an uncoupling effect on mitochondrial OXPHOS (Wojtczak and Schonfeld, 1993), the optimal concentration of octanoyl-l-carnitine was determined in each muscle sample by titration. After the addition of permeabilized fibers (approximately 1.5–3.0 mg of gastrocnemius muscle) to the chamber in the respirometer filled with 2 ml of MiR05, the substrates, ADP, and cytochrome *c* were added in the following order.

(*1*) malate (2 mmol/l) + octanoyl-l-carnitine (0.15 mmol/l), (*2*) ADP (5 mmol/l), (*3*) glutamate (10 mmol/l; a complex I-linked substrate), (*4*) pyruvate (10 mmol/l; a complex I-linked substrate), and (*5*) cytochrome *c* (10 μmol/l), (*6*) succinate (10 μmol/l; a complex II-linked substrate).

Mitochondrial coupling states were distinguished as LEAK (without ADP) and OXPHOS (saturating ADP). The integrity of the outer mitochondrial membrane was tested by adding cytochrome *c*, and data were eliminated when the increase in oxygen consumption rate was > 10%, which was a sign of outer mitochondrial membrane damage. Respiratory rates (i.e., O_2 consumption rates) were expressed as the O_2 flux normalized to muscle weight (pmol/sec/mg wet weight of muscle tissue).

2.8. Immunoblotting

Immunoblotting was performed as described previously (Fukushima et al., 2014; Maekawa et al., 2019; Matsumoto et al., 2018; Nishikawa et al., 2015; Ono et al., 2015). Hindlimb skeletal muscle tissue samples were homogenized in 1 × Cell Lysis Buffer (Cell Signaling Technology, Danvers, MA) supplemented with 1 × Complete Protease Inhibitor Cocktail (Roche, Basel, Switzerland) and 1 mmol/L phenylmethylsulfonyl fluoride. After sonification and centrifugation at 15,000 *g* for 20 min at 4 ˚C, the supernatants were collected. Protein aliquots were taken for the total protein assay (Pierce BCA, Rockford, IL). The remaining lysate (20 μg) was added onto 10% polyacrylamide gels (Bio-Rad, Hercules, CA), electrophoretically separated by sodium dodecyl sulfate-polyacrylamide gel electrophoresis using running buffer, and then transferred by electroblotting to a polyvinylidene fluoride membrane (Bio-Rad) using transfer buffer at 20 V, overnight.

After being blocked in TBS buffer with 0.1% Tween-20 (TBST) in 5% nonfat dry milk or 5% albumin, the membranes were incubated overnight at 4 ˚C with primary antibodies (dilution 1:1000) against the phosphorylated forms of AMP-activated protein kinase α (AMPKα) Thr^{172}, total AMPKα (Cell Signaling Technology), peroxisome proliferator-activated receptor gamma coactivator-1 (PGC-1), CD36, carnitine palmitoyltransferase (CPT)1b, electron transfer flavoprotein (ETF)A, ETFB, long-chain specific acyl-CoA dehydrogenase (ACADL), and enoyl-CoA hydratase and 3-hydroxyacyl CoA dehydrogenase (EHHADH) (Abcam). After washing 3 times in TBST buffer, the membranes were incubated with secondary antibodies conjugated with horseradish peroxidase (HRP, dilution 1:5000; Abcam).

Membranes were washed again in TBST and incubated with the chemiluminescence detection reagent ECL™ or the ECL prime Western Blotting Analysis System (GE Healthcare, Amersham, UK) to enhance their chemiluminescence. Equal loading of protein was verified by Ponceau-S staining (Beacle, Kyoto, Japan). Quantification of protein levels was performed with Image J software (U.S. National Institutes of Health, Bethesda, MD).

2.9. Statistical analysis

Data are presented as the mean ± S.E.M. For multiple-group comparisons, one-way ANOVA followed by the Tukey test was performed. Survival analysis was performed by the Kaplan-Meier method, and between-group differences in survival were tested using the log-rank test. A *P*-value of less than 0.05 was considered to indicate a

Table 1
Characteristics of the mice.

	Sham	HF	HF + Empa
Body and organ weights:			
N	8	7	7
BW, g	27.2 ± 0.4	27.5 ± 0.4	26.3 ± 0.4
Heart weight/BW, mg/g	4.1 ± 0.04	5.7 ± 0.4*	5.1 ± 0.4
LV weight/BW, mg/g	3.0 ± 0.1	3.8 ± 0.1*	3.5 ± 0.2*
Lung weight/BW, mg/g	5.0 ± 0.1	6.1 ± 0.6	6.3 ± 0.6
Lower limb skeletal muscle/BW, mg/g	14.0 ± 0.3	14.2 ± 0.3	13.7 ± 0.2
Echocardiography:			
N	8	7	7
Heart rate, beats/min	691 ± 8	651 ± 10	633 ± 18
LV EDD, mm	3.3 ± 0.1	5.3 ± 0.2*	5.0 ± 0.3*
LV ESD, mm	1.4 ± 0.1	4.4 ± 0.2*	4.1 ± 0.3*
Fractional shortening, %	57.5 ± 3.1	17.9 ± 1.8*	19.1 ± 1.9*
AWT, mm	0.79 ± 0.03	0.30 ± 0.02*	0.33 ± 0.02*
PWT, mm	0.81 ± 0.02	1.01 ± 0.02*	0.96 ± 0.07*
Behavioral measurements:			
N	11	9	10
Physical activity, count/day	3.702 ± 1000	3262 ± 617	2617 ± 365
Histological analysis (skeletal muscle)			
N	6	7	5
Cross-sectional area,/μm^2	2020 ± 60	2084 ± 62	1810 ± 112

Values are mean ± SE; *$p < 0.05$ vs. sham; †$p < 0.05$ vs. HF. AWT: anterior wall thickness, BW: body weight, EDD: end-diastolic diameter, Empa: empagliflozin, ESD: end-systolic diameter, HF: heart failure, LV: left ventricular, N: no. of mice, PWT: posterior wall thickness.

statistically significant difference between 2 groups.

3. Results

There was no significant difference in the mortality rate between the HF and HF + Empa mice up to 6 weeks after the operation (56.3% and 62.5%). None of the mice receiving the sham operation died. There was no significant difference in food intake (sham vs. HF vs. HF + Empa, 4.8 ± 0.5 vs. 4.4 ± 0.7 vs. 4.0 ± 0.3 g/day, respectively) among the 3 groups. According to the actual food intake of the mice, Empa was administered to HF mice at 34.8–42.3 mg/kg/day.

3.1. Characteristics of the mice

Table 1 summarizes the characteristics of the mice. The heart weight/BW, the left ventricular (LV) weight/BW, and lung weight/BW values were significantly increased in the HF mice compared with the sham-operated mice. LV diameter and posterior wall thickness were significantly greater, and LV fractional shortening was significantly lower in the HF mice compared with the sham mice. There was no significant difference in heart rate between the sham and HF mice. Administration of the SGLT2 inhibitor Empa did not improve the heart weight/BW, LV weight/BW, lung weight/BW, or any of the above-mentioned echocardiographic alterations of the HF mice. There were no significant differences in the weights of the lower-limb skeletal muscles, including the quadriceps, gastrocnemius, and soleus muscles (Table 1) or in the muscle cell cross-sectional area of the gastrocnemius muscle among the sham, HF, and HF + Empa mice (Table 1, Suppl. Fig. 1).

3.2. Urinary/blood glucose levels and serum insulin levels

There was no significant difference in urinary (Fig. 2A) or blood (Fig. 2B) glucose levels or serum insulin levels (Fig. 2C) between the HF mice and sham mice. As expected, the addition of Empa to the diet significantly increased urinary glucose levels in the HF mice, but no difference in blood glucose and serum insulin levels was observed (Fig. 2B, C).

3.3. Exercise endurance capacity, muscle strength, and spontaneous physical activity

Intriguingly, the exercise endurance capacity evaluated by the four-limb hang time was significantly reduced in the HF mice but was ameliorated in the HF + Empa mice (Fig. 3A, B). On the other hand, there was no difference in muscle endurance between sham and sham + Empa (sham 9382 ± 1605 vs. sham + Empa 6992 ± 1932 s, $P = 0.43$). Therefore, we excluded the sham + Empa group from the following analysis. In contrast to muscle endurance, the skeletal muscle strength assessed by the grip strength test and spontaneous physical activity were similar among 3 groups (Fig. 3C, D and Table 1).

3.4. Fat weight, serum free fatty acid level, and serum β-OHB level

There was no significant difference in EWAT weights/BW or serum FFA and serum β-OHB levels between the HF mice and sham mice (Fig. 4). Empa significantly decreased the EWAT weights and increased serum FFA and β-OHB levels in the HF mice (Fig. 4).

3.5. Mitochondrial OXPHOS capacity measured using fatty acid substrates in permeabilized fibers

Fig. 5A shows representative graphs of mitochondrial respiratory capacity measured using fatty acid substrates of skeletal muscle in HF and HF + Empa mice. We used malate as the non-fatty acid substrate and octanoyl-l-carnitine as the fatty acid substrate. Non-ADP-stimulated LEAK respiration normalized to muscle weight did not differ significantly among the 3 groups (Fig. 5B). ADP-stimulated OXPHOS respiration was significantly decreased in the HF mice, and was ameliorated by Empa (Fig. 5B).

After the addition of glutamate and pyruvate, the same OXPHOS respiration results were observed (Fig. 5B). However, after the addition of succinate as a substrate of complex II and rotenone as an inhibitor of complex I, ADP-stimulated OXPHOS respiration was significantly decreased in the HF mice, and this decrease was ameliorated by Empa (Fig. 5B).

3.6. Fatty acid oxidation-associated protein levels in skeletal muscle

To clarify the mechanism by which impaired mitochondrial fatty acid oxidation was ameliorated by Empa, we analyzed the levels of proteins associated with fatty acid uptake and oxidation in the skeletal muscle. Supplemental Fig. 2 shows representative blots (panel A) and densitometric quantification (panel B). There were no significant differences in protein expression associated with the master transcriptional factor (PGC-1α) or the energy sensor (AMPK) among the 3 groups. Similarly, the expression of proteins involved in cellular and mitochondrial fatty acid uptake (CD36 and CPT1B), the electron transport chain (ETFA and ETFB), and fatty acid β-oxidation enzymes (ACADL and EHHAD) were not significantly different among the groups.

4. Discussion

Impaired skeletal muscle function is one of the clinical features in HF patients, which is considered the primary mechanism of these patients' easy fatigability and exercise intolerance. This mechanism includes impaired energy metabolism and oxidative enzymes (Haykowsky et al., 2014; Kinugawa et al., 2015; Kitzman et al., 2014; Matsumoto et al., 2018; Molina et al., 2016; Takada et al., 2016; Tsuda et al., 2018). Our present study demonstrated several novel observations regarding the effects of Empa on skeletal muscle abnormalities associated with HF. Notably, Empa improved the exercise endurance capacity of HF mice without affecting any of their cardiac functions post-MI. The beneficial effect of Empa on endurance capacity is

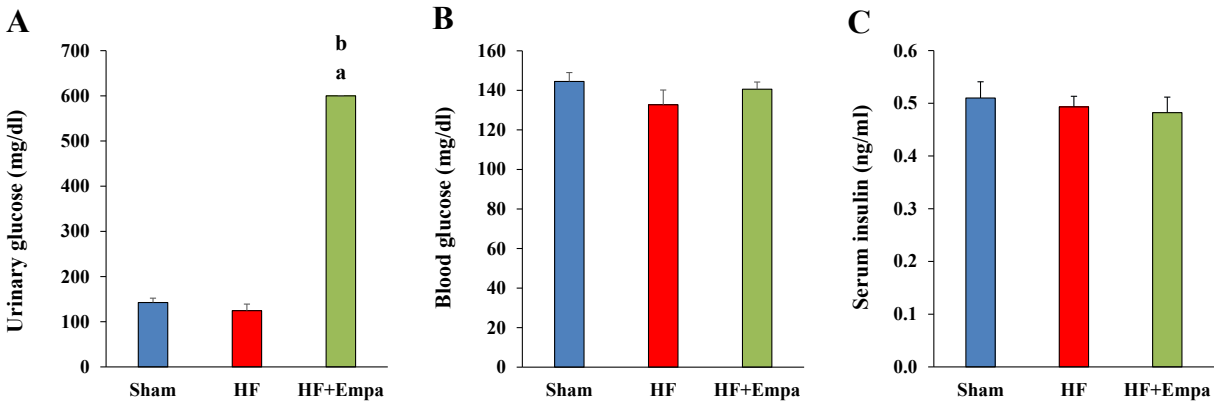

Fig. 2. Empagliflozin increases urinary glucose levels without affecting blood glucose or serum insulin levels
Summarized data of urinary glucose (**A**), blood glucose (**B**), and serum insulin (**C**) (n = 7–8 for each group) of the sham, HF, and HF + Empa mice. Data are the mean ± S.E.M. $^{a}P < 0.05$ vs. sham; $^{b}P < 0.05$ vs. HF. Empa: empagliflozin, HF: heart failure.

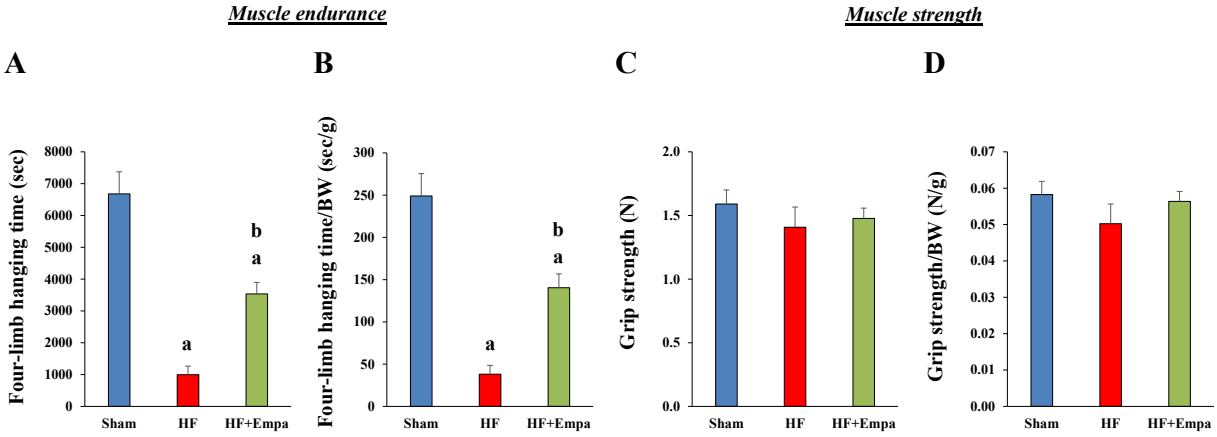

Fig. 3. Empagliflozin ameliorates the reduced endurance capacity in a murine model of heart failure
Summarized data of four-limb hanging time (**A**), four-limb hanging time/BW (**B**), grip strength (**C**), and grip strength/BW (**D**) (n = 6–10 for each group) in the sham, HF, and HF + Empa mice. Data are mean ± S.E.M. $^{a}P < 0.05$ vs. sham; $^{b}P < 0.05$ vs. HF.

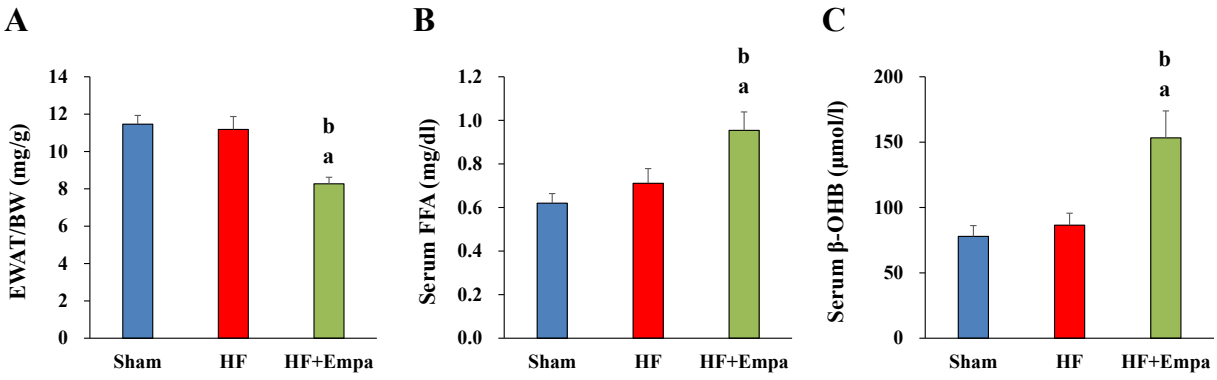

Fig. 4. Empagliflozin augments serum free fatty acid and β-hydroxybutyrate levels while reducing adipose tissue weight
Summarized data of the EWAT/BW (**A**), serum FFA (**B**), and serum β-OHB (**C**) (n = 7–8, each group) in the sham, HF, and HF + Empa mice. Data are shown as the mean ± S.E.M. $^{a}P < 0.05$ vs. sham; $^{b}P < 0.05$ vs. MI. β-OHB: beta-hydroxybutyrate, BW: body weight; EWAT: epididymal white adipose tissue, FFA: free fatty acid.

associated with the amelioration of impaired fatty acid oxidation in muscle mitochondria of HF mice.

Sano et al. reported that maximal hand-grip strength is increased after SGLT2 inhibitor treatment in patients with type 2 diabetes (Sano et al., 2016). The putative mechanisms responsible for the beneficial effects of SGLT2 inhibition on maximal hand-grip strength may include improved mitochondrial function. As these subjects were well educated about appropriate exercise therapy, the improved muscle strength in diabetic patients may be attributed to increased spontaneous physical activity after SGLT2 inhibitor treatment. In our present study, we clearly showed that Empa did not affect muscle strength and spontaneous physical activity in HF mice. Therefore, our results may indicate that the improvement of exercise endurance capacity by Empa is attributed to the enhancement of fatty acid oxidation in skeletal muscle.

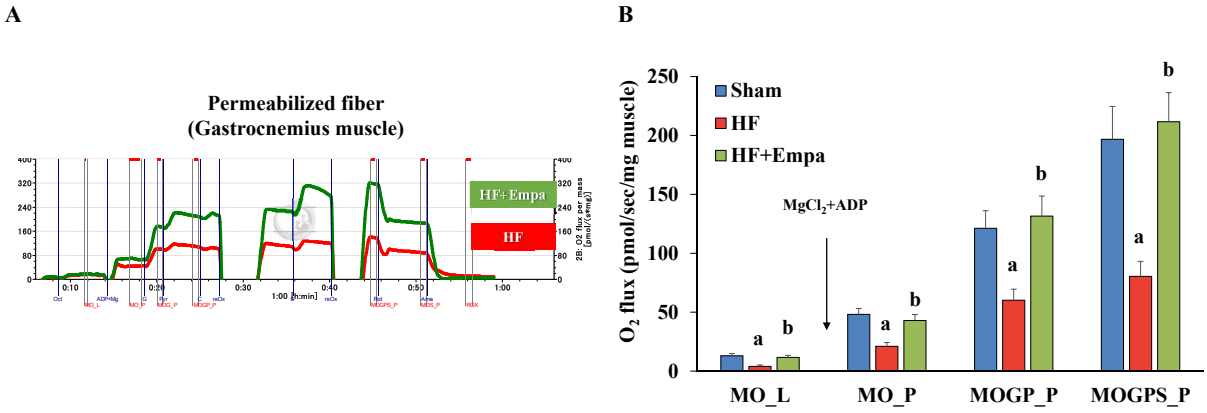

Fig. 5. Empagliflozin restores impaired mitochondrial fatty acid oxidation in the skeletal muscle of post-MI heart failure mice
Representative O_2 flux (**A**, *lower red line*: HF; *upper green line*: HF + Empa), and summarized data (**B**) of mitochondrial respiration with fatty acid substrates in the gastrocnemius muscle of sham, HF, and HF + Empa mice. Data are shown as the mean ± S.E.M. n = 5–6 for each group. $^{a}P < 0.05$ vs. sham; $^{b}P < 0.05$ vs. HF. ADP: adenosine diphosphate, G: glutamate, M: malate, O: octanoyl-l-carnitine, P: pyruvate, S: succinate.

Consistent with previous reports demonstrating lipolysis in adipose tissue of mice treated with SGLT2 inhibitors (Devenny et al., 2012; Yokono et al., 2014), we found that the administration of Empa reduced visceral fat and increased blood levels of fatty acids in HF mice. Our findings suggest that the mechanism underlying the reduction in fat weight partially depends on increased energy expenditure and enhanced fatty acid oxidation. A recent study reported that Empa enhances the phosphorylation of AMPKα in skeletal muscle in a type 2 diabetic mouse model (Xu et al., 2017). Moreover, a similar study found that canagliflozin activates AMPK *in vitro* and lowers liver lipid content (Hawley et al., 2016). To our surprise, the molecular lines of evidence, including AMPK protein levels, failed to support this effect of Empa, suggesting that post-translational modifications caused by Empa may play a predominant role in this phenomenon.

Consistent with previous studies (Hamasaki, 2018; Obata et al., 2016), Empa increased blood β-OHB levels in HF mice in the present study. β-OHB oxidation produces acetyl CoA, which in turn can promote acetylation, a novel post-translational modification, via a non-enzymatic reaction (Davies et al., 2016). Indeed, recent studies have shown that increased ketone body oxidation as well as β-OHB oxidation is evident in failing hearts, accompanied by the increased acetylation of various metabolic pathways (Aubert et al., 2016; Horton et al., 2016). Lysine acetylation has emerged as an important regulator for mitochondrial energy metabolism (Overmyer et al., 2015; Pougovkina et al., 2014; Shimazu et al., 2010). Although numerous metabolic enzymes that are involved in fatty acid β-oxidation, glycolysis, and the tricarboxylic acid cycle can be acetylated, resulting in the activation or inhibition of enzymatic activities, fatty acid β-oxidation enzymes appear to be a main target for acetylation. (Fukushima and Lopaschuk, 2016; Thapa et al., 2017). We previously reported that the hyperacetylation of fatty acid β-oxidation enzymes enhances actual fatty acid oxidation rates through positive regulation of their enzyme activities in obese HF mice as well as in the hearts of newborn rabbit (Fukushima et al., 2016a; Sankaralingam et al., 2015). More recently, we demonstrated that the acetylation of fatty acid β-oxidation enzymes is an indispensable process for the substantial maturational increase in cardiac fatty acid oxidation post-birth (Fukushima et al., 2018). Despite the possible mechanisms described above, the HF + Empa group did not improve muscle endurance capacity to the same extent as the sham group (Fig. 3). Therefore, other factor(s) except skeletal muscle mitochondrial function, muscle volume, and strength that were not different between HF groups in this study may also play an important role controlling skeletal muscle function. Recent clinical studies have shown that Empagliflozin improves cardiorespiratory fitness in patients with diabetes (Kumar et al., 2018) and patients with HF associated with diabetes (Carbone et al., 2018; Nunez et al., 2018). These data can explain the favorable effects of Empagliflozin on cardiovascular outcomes in patients with diabetes. In these reports, the beneficial effects of Empagliflozin on cardiorespiratory fitness were suggested to be due to the inhibition of renin-angiotensin system by fluid reduction or the increased cardiac output by afterload reduction. While these things are likely to be true, Empagliflozin has been known to have the action beyond an improvement in hemodynamics. Furthermore, it is still unknown whether an SGLT2 inhibitor is directly effective for HF patients without diabetes. Thus, our results may help to interpret the effects of SGLT2 inhibitors on HF.

Collectively, these findings suggest that increased β-OHB levels as a result of the administration of Empa may promote the hyperacetylation of fatty acid β-oxidation enzymes, resulting in the enhancement of fatty acid oxidation in skeletal muscle. Further research focusing on post-translation control via Empa will provide novel mechanistic insights into the beneficial effects of Empa for the reduction of rehospitalization and mortality of HF patients observed in the EMPA-REG OUTCOME trial (Zinman et al., 2015). Clinical relevance of our model remains unknown. However, our model reproduces very well the skeletal muscle abnormalities observed in patients with HF (Matsumoto et al., 2018; Takada et al., 2016; Tsuda et al., 2018). Our present study shed light on the efficacy of Empagliflozin targeted to exercise intolerance and skeletal muscle abnormalities for patients with HF. The application of our results to clinical study is desired.

Given the observational nature of this study, there are several limitations that should be noted. First, although our *in vivo* data are generally solid, cause-and-effect relationships between blood β-OHB levels and impaired fatty acid oxidation or lowered exercise capacity remain to be determined. Specifically, the lack of any lines of evidence regarding whether β-OHB could ultimately affect mitochondrial respiration is a major limitation of our study. We were also unable to determine the correlation between β-OHB and mitochondrial respiration in the skeletal muscle, owing to a technical limitation. To gain direct lines of evidence of the role of β-OHB in the regulation of muscle fatty acid oxidation, further studies using mice with muscle-specific ketone oxidation deficiency are necessary. Second, the downstream mechanism by which skeletal muscle mitochondrial respiration with fatty acids is reduced remains to be elucidated. It is also unknown as to how β-OHB acts on skeletal muscle abnormalities.

The EMPA-REG OUTCOME trial demonstrated significant reductions in cardiovascular death and HF hospitalization risk in patients with type 2 diabetes mellitus using the SGLT2 inhibitor Empa. Although Empa has been reported to prevent the worsening of cardiac function in transverse aortic constriction mice (Byrne et al., 2017), this mechanism

is not definitive as SGLT2 receptors are known to be absent in the heart (Sabolic et al., 2012), Moreover, clinical lines of evidence on improved cardiac function by SGLT2 inhibitors has never been documented. Rather, the administration of an SGLT2 inhibitor appears to ameliorate multiple organ abnormalities associated with HF through metabolic modulation. We clearly demonstrated that Empa improved exercise endurance capacity in a mouse model of HF via the enhancement of fatty acid oxidation in skeletal muscle. As exercise capacity is a well-known predictor of adverse outcomes of HF, our results may demonstrate one of the mechanisms involved in the beneficial effects of SGLT2 inhibitors shown in clinical trials.

5. Conclusions

Empa, an SGLT2 inhibitor, improved exercise endurance and normalized fatty acid oxidation in the skeletal muscle of post-MI HF mice. Importantly, these beneficial effects of Empa on exercise endurance were independent of glucose metabolism and cardiac function. SGLT2 inhibitors may hence be novel therapeutic agents against skeletal muscle dysfunction in HF.

Author contributions

All experiments were conducted at the Department of Cardiovascular Medicine, Faculty of Medicine and Graduate School of Medicine, Hokkaido University. H.N., S.T., and A.F. conceived and designed the research. H.N., S.T., J.M., A.F., N.K., S.M., R.S., I.N., T.F., K.T., K.Y., O.Y., and A.S. performed the experiments. H.N., S.T., and J.M. analyzed the data. T.Y. and S.K. interpreted the results of the experiments. H.N., S.T., A.F., and S.K. drafted the manuscript. T.F. and T.Y. edited and revised the manuscript. All authors approved the final version of the manuscript and agree to be accountable for all aspects of the work in ensuring that questions associated with the accuracy or integrity of any part of the work are appropriately investigated and resolved. All persons designated as authors qualify for authorship, and all those who qualify for authorship are listed.

Sources of funding

This work was supported in part by grants from the Japanese Grants-in-Aid for Scientific Research (JP17K15979 (to T.F.), JP17K10137 (to A.F.), and JP17H04758 (to S.T.), 18H03187 (to S.K.), Grant-in-Aid for Challenging Exploratory Research (19K22791 [to S.T.], the Japan Foundation for Applied Enzymology (to S.T.), a Hokkaido Heart Association Grant for Research (to S.T.), the MSD Life Science Foundation (to S.T.), the Uehara Memorial Foundation (to S.T.), the Cardiovascular Research Fund, Tokyo, Japan (to S.T.), the Fukuda Memorial Foundation for Medical Research (to S.T.), a Kimura Memorial Heart Foundation Research Grant for 2017 (to S.T.), the SENSHIN Medical Research Foundation (to S.T.), the Nakatomi Foundation (to S.T.), the Japan Heart Foundation (to S.T.), a Sasakawa Scientific Research Grant from The Japan Science Society (to S.T.), and the Center of Innovation Program from the Japan Science and Technology Agency.

Disclosures

The authors state that there are no disclosures associated with this study.

Declaration of competing interest

This study was supported by grants from Boehringer Ingelheim. Empagliflozin was provided by Boehringer Ingelheim.

Acknowledgments

The authors thank Yuki Kimura and Miwako Yamane for their technical assistance, and Misaki Kihara, Naoko Toshiro, Tsukusu Yamanaka, and Misato Kobayashi for secretarial support, and H.A. Popiel for her critical reading of the manuscript.

Appendix A. Supplementary data

Supplementary data to this article can be found online at https://doi.org/10.1016/j.ejphar.2019.172810.

References

Abbate, A., Van Tassell, B.W., Canada, J.M., Dixon, D.L., Arena, R.A., Biondi-Zoccai, G., 2015. Pharmacologic and surgical interventions to improve functional capacity in heart failure. Heart Fail. Clin. 11, 117–124.

Aubert, G., Martin, O.J., Horton, J.L., Lai, L., Vega, R.B., Leone, T.C., Koves, T., Gardell, S.J., Kruger, M., Hoppel, C.L., Lewandowski, E.D., Crawford, P.A., Muoio, D.M., Kelly, D.P., 2016. The failing heart relies on ketone bodies as a fuel. Circulation 133, 698–705.

Byrne, N.J., Parajuli, N., Levasseur, J.L., Boisvenue, J., Beker, D.L., Masson, G., Fedak, P.W.M., Verma, S., Dyck, J.R.B., 2017. Empagliflozin prevents worsening of cardiac function in an experimental model of pressure overload-induced heart failure. JACC Basic Transl. Med. 2, 347–354.

Camporez, J.P., Petersen, M.C., Abudukadier, A., Moreira, G.V., Jurczak, M.J., Friedman, G., Haqq, C.M., Petersen, K.F., Shulman, G.I., 2016. Anti-myostatin antibody increases muscle mass and strength and improves insulin sensitivity in old mice. Proc. Natl. Acad. Sci. U.S.A. 113, 2212–2217.

Carbone, S., Canada, J.M., Billingsley, H.E., Kadariya, D., Dixon, D.L., Trankle, C.R., Buckley, L.F., Markley, R., Vo, C., Medina de Chazal, H., Christopher, S., Buzzetti, R., Van Tassell, B.W., Abbate, A., 2018. Effects of empagliflozin on cardiorespiratory fitness and significant interaction of loop diuretics. Diabetes Obes. Metab. 20, 2014–2018.

Davies, M.N., Kjalarsdottir, L., Thompson, J.W., Dubois, L.G., Stevens, R.D., Ilkayeva, O.R., Brosnan, M.J., Rolph, T.P., Grimsrud, P.A., Muoio, D.M., 2016. The acetyl group buffering action of carnitine acetyltransferase offsets macronutrient-induced lysine acetylation of mitochondrial proteins. Cell Rep. 14, 243–254.

Devenny, J.J., Godonis, H.E., Harvey, S.J., Rooney, S., Cullen, M.J., Pelleymounter, M.A., 2012. Weight loss induced by chronic dapagliflozin treatment is attenuated by compensatory hyperphagia in diet-induced obese (DIO) rats. Obesity 20, 1645–1652.

Fukushima, A., Alrob, O.A., Zhang, L., Wagg, C.S., Altamimi, T., Rawat, S., Rebeyka, I.M., Kantor, P.F., Lopaschuk, G.D., 2016a. Acetylation and succinylation contribute to maturational alterations in energy metabolism in the newborn heart. Am. J. Physiol. Heart Circ. Physiol. 311, H347–H363.

Fukushima, A., Kinugawa, S., Takada, S., Matsumoto, J., Furihata, T., Mizushima, W., Tsuda, M., Yokota, T., Matsushima, S., Okita, K., Tsutsui, H., 2016b. Direct renin inhibitor ameliorates insulin resistance by improving insulin signaling and oxidative stress in the skeletal muscle from post-infarct heart failure in mice. Eur. J. Pharmacol. 779, 147–156.

Fukushima, A., Kinugawa, S., Takada, S., Matsushima, S., Sobirin, M.A., Ono, T., Takahashi, M., Suga, T., Homma, T., Masaki, Y., Furihata, T., Kadoguchi, T., Yokota, T., Okita, K., Tsutsui, H., 2014. (Pro)renin receptor in skeletal muscle is involved in the development of insulin resistance associated with postinfarct heart failure in mice. Am. J. Physiol. Endocrinol. Metab. 307, E503–E514.

Fukushima, A., Lopaschuk, G.D., 2016. Cardiac fatty acid oxidation in heart failure associated with obesity and diabetes. Biochim. Biophys. Acta 1861, 1525–1534.

Fukushima, A., Zhang, L., Huqi, A., Lam, V.H., Rawat, S., Altamimi, T., Wagg, C.S., Dhaliwal, K.K., Hornberger, L.K., Kantor, P.F., Rebeyka, I.M., Lopaschuk, G.D., 2018. Acetylation contributes to hypertrophy-caused maturational delay of cardiac energy metabolism. JCI Insight 3.

Goda, A., Lund, L.H., Mancini, D., 2011. The Heart Failure Survival Score outperforms the peak oxygen consumption for heart transplantation selection in the era of device therapy. J. Heart Lung Transplant. 30, 315–325.

Hamasaki, H., 2018. Effects of glucose-lowering agents on cardiorespiratory fitness. World J. Diabetes 9, 230–238.

Hawley, S.A., Ford, R.J., Smith, B.K., Gowans, G.J., Mancini, S.J., Pitt, R.D., Day, E.A., Salt, I.P., Steinberg, G.R., Hardie, D.G., 2016. The Na+/Glucose cotransporter inhibitor canagliflozin activates AMPK by inhibiting mitochondrial function and increasing cellular AMP levels. Diabetes 65, 2784–2794.

Haykowsky, M.J., Kouba, E.J., Brubaker, P.H., Nicklas, B.J., Eggebeen, J., Kitzman, D.W., 2014. Skeletal muscle composition and its relation to exercise intolerance in older patients with heart failure and preserved ejection fraction. Am. J. Cardiol. 113, 1211–1216.

Horton, J.L., Martin, O.J., Lai, L., Riley, N.M., Richards, A.L., Vega, R.B., Leone, T.C., Pagliarini, D.J., Muoio, D.M., Bedi Jr., K.C., Margulies, K.B., Coon, J.J., Kelly, D.P., 2016. Mitochondrial protein hyperacetylation in the failing heart. JCI Insight 2.

Kinugawa, S., Takada, S., Matsushima, S., Okita, K., Tsutsui, H., 2015. Skeletal muscle abnormalities in heart failure. Int. Heart J. 56, 475–484.

Kitzman, D.W., Nicklas, B., Kraus, W.E., Lyles, M.F., Eggebeen, J., Morgan, T.M., Haykowsky, M., 2014. Skeletal muscle abnormalities and exercise intolerance in

older patients with heart failure and preserved ejection fraction. Am. J. Physiol. Heart Circ. Physiol. 306, H1364–H1370.
Kosmala, W., Rojek, A., Przewlocka-Kosmala, M., Wright, L., Mysiak, A., Marwick, T.H., 2016. Effect of aldosterone antagonism on exercise tolerance in heart failure with preserved ejection fraction. J. Am. Coll. Cardiol. 68, 1823–1834.
Kumar, N., Garg, A., Bhatt, D.L., Sabongui, S., Gupta, N., Chaudhry, S., Arena, R., Verma, S., 2018. Empagliflozin improves cardiorespiratory fitness in type 2 diabetes: translational implications. Can. J. Physiol. Pharmacol. 96, 1184–1187.
Lin, B., Koibuchi, N., Hasegawa, Y., Sueta, D., Toyama, K., Uekawa, K., Ma, M., Nakagawa, T., Kusaka, H., Kim-Mitsuyama, S., 2014. Glycemic control with empagliflozin, a novel selective SGLT2 inhibitor, ameliorates cardiovascular injury and cognitive dysfunction in obese and type 2 diabetic mice. Cardiovasc. Diabetol. 13, 148.
Lytvyn, Y., Bjornstad, P., Udell, J.A., Lovshin, J.A., Cherney, D.Z.I., 2017. Sodium glucose cotransporter-2 inhibition in heart failure: potential mechanisms, clinical applications, and summary of clinical trials. Circulation 136, 1643–1658.
Maekawa, S., Takada, S., Nambu, H., Furihata, T., Kakutani, N., Setoyama, D., Ueyanagi, Y., Kang, D., Sabe, H., Kinugawa, S., 2019. Linoleic acid improves assembly of the CII subunit and CIII2/CIV complex of the mitochondrial oxidative phosphorylation system in heart failure. Cell Commun. Signal. 17, 128.
Matsumoto, J., Takada, S., Kinugawa, S., Furihata, T., Nambu, H., Kakutani, N., Tsuda, M., Fukushima, A., Yokota, T., Tanaka, S., Takahashi, H., Watanabe, M., Hatakeyama, S., Matsumoto, M., Nakayama, K.I., Otsuka, Y., Sabe, H., Tsutsui, H., Anzai, T., 2018. Brain-derived neurotrophic factor improves limited exercise capacity in mice with heart failure. Circulation 138, 2064–2066.
Molina, A.J., Bharadwaj, M.S., Van Horn, C., Nicklas, B.J., Lyles, M.F., Eggebeen, J., Haykowsky, M.J., Brubaker, P.H., Kitzman, D.W., 2016. Skeletal muscle mitochondrial content, oxidative capacity, and Mfn2 expression are reduced in older patients with heart failure and preserved ejection fraction and are related to exercise intolerance. JACC Heart Fail 4, 636–645.
Nishikawa, M., Ishimori, N., Takada, S., Saito, A., Kadoguchi, T., Furihata, T., Fukushima, A., Matsushima, S., Yokota, T., Kinugawa, S., Tsutsui, H., 2015. AST-120 ameliorates lowered exercise capacity and mitochondrial biogenesis in the skeletal muscle from mice with chronic kidney disease via reducing oxidative stress. Nephrol. Dial. Transplant. 30, 934–942.
Nunez, J., Palau, P., Dominguez, E., Mollar, A., Nunez, E., Ramon, J.M., Minana, G., Santas, E., Facila, L., Gorriz, J.L., Sanchis, J., Bayes-Genis, A., 2018. Early effects of empagliflozin on exercise tolerance in patients with heart failure: a pilot study. Clin. Cardiol. 41, 476–480.
Obata, A., Kubota, N., Kubota, T., Iwamoto, M., Sato, H., Sakurai, Y., Takamoto, I., Katsuyama, H., Suzuki, Y., Fukazawa, M., Ikeda, S., Iwayama, K., Tokuyama, K., Ueki, K., Kadowaki, T., 2016. Tofogliflozin improves insulin resistance in skeletal muscle and accelerates lipolysis in adipose tissue in male mice. Endocrinology 157, 1029–1042.
Okita, K., Kinugawa, S., Tsutsui, H., 2013. Exercise intolerance in chronic heart failure–skeletal muscle dysfunction and potential therapies. Circ. J. 77, 293–300.
Ono, T., Takada, S., Kinugawa, S., Tsutsui, H., 2015. Curcumin ameliorates skeletal muscle atrophy in type 1 diabetic mice by inhibiting protein ubiquitination. Exp. Physiol. 100, 1052–1063.
Overmyer, K.A., Evans, C.R., Qi, N.R., Minogue, C.E., Carson, J.J., Chermside-Scabbo, C.J., Koch, L.G., Britton, S.L., Pagliarini, D.J., Coon, J.J., Burant, C.F., 2015. Maximal oxidative capacity during exercise is associated with skeletal muscle fuel selection and dynamic changes in mitochondrial protein acetylation. Cell Metabol. 21, 468–478.
Pougovkina, O., te Brinke, H., Ofman, R., van Cruchten, A.G., Kulik, W., Wanders, R.J., Houten, S.M., de Boer, V.C., 2014. Mitochondrial protein acetylation is driven by acetyl-CoA from fatty acid oxidation. Hum. Mol. Genet. 23, 3513–3522.
Rebo, J., Mehdipour, M., Gathwala, R., Causey, K., Liu, Y., Conboy, M.J., Conboy, I.M., 2016. A single heterochronic blood exchange reveals rapid inhibition of multiple tissues by old blood. Nat. Commun. 7, 13363.
Sabolic, I., Vrhovac, I., Eror, D.B., Gerasimova, M., Rose, M., Breljak, D., Ljubojevic, M., Brzica, H., Sebastiani, A., Thal, S.C., Sauvant, C., Kipp, H., Vallon, V., Koepsell, H., 2012. Expression of Na+-D-glucose cotransporter SGLT2 in rodents is kidney-specific and exhibits sex and species differences. Am. J. Physiol. Cell Physiol. 302, C1174–C1188.
Sankaralingam, S., Abo Alrob, O., Zhang, L., Jaswal, J.S., Wagg, C.S., Fukushima, A., Padwal, R.S., Johnstone, D.E., Sharma, A.M., Lopaschuk, G.D., 2015. Lowering body weight in obese mice with diastolic heart failure improves cardiac insulin sensitivity and function: implications for the obesity paradox. Diabetes 64, 1643–1657.
Sano, M., Meguro, S., Kawai, T., Suzuki, Y., 2016. Increased grip strength with sodium-glucose cotransporter 2. J. Diabetes 8, 736–737.
Shimazu, T., Hirschey, M.D., Hua, L., Dittenhafer-Reed, K.E., Schwer, B., Lombard, D.B., Li, Y., Bunkenborg, J., Alt, F.W., Denu, J.M., Jacobson, M.P., Verdin, E., 2010. SIRT3 deacetylates mitochondrial 3-hydroxy-3-methylglutaryl CoA synthase 2 and regulates ketone body production. Cell Metabol. 12, 654–661.
Sobirin, M.A., Kinugawa, S., Takahashi, M., Fukushima, A., Homma, T., Ono, T., Hirabayashi, K., Suga, T., Azalia, P., Takada, S., Taniguchi, M., Nakayama, T., Ishimori, N., Iwabuchi, K., Tsutsui, H., 2012. Activation of natural killer T cells ameliorates postinfarct cardiac remodeling and failure in mice. Circ. Res. 111, 1037–1047.
Tahara, A., Takasu, T., Yokono, M., Imamura, M., Kurosaki, E., 2016. Characterization and comparison of sodium-glucose cotransporter 2 inhibitors in pharmacokinetics, pharmacodynamics, and pharmacologic effects. J. Pharmacol. Sci. 130, 159–169.
Takaaki Furihata, S.K., Takada, Shingo, Fukushima, Arata, Takahashi, Masashige, Homma, Tsuneaki, Masaki, Yoshihiro, Tsuda, Masaya, Matsumoto, Junichi, Mizushima, Wataru, Matsushima, Shouji, Yokota, Takashi, Tsutsui, Hiroyuki, 2016. The experimental model of transition from compensated cardiac hypertrophy to failure created by transverse aortic constriction in mice. IJC Heart Vasculature 11, 24–28.
Takada, S., Masaki, Y., Kinugawa, S., Matsumoto, J., Furihata, T., Mizushima, W., Kadoguchi, T., Fukushima, A., Homma, T., Takahashi, M., Harashima, S., Matsushima, S., Yokota, T., Tanaka, S., Okita, K., Tsutsui, H., 2016. Dipeptidyl peptidase-4 inhibitor improved exercise capacity and mitochondrial biogenesis in mice with heart failure via activation of glucagon-like peptide-1 receptor signalling. Cardiovasc. Res. 111, 338–347.
Thapa, D., Zhang, M., Manning, J.R., Guimaraes, D.A., Stoner, M.W., O'Doherty, R.M., Shiva, S., Scott, I., 2017. Acetylation of mitochondrial proteins by GCN5L1 promotes enhanced fatty acid oxidation in the heart. Am. J. Physiol. Heart Circ. Physiol. 313, H265–h274.
Tsuda, M., Fukushima, A., Matsumoto, J., Takada, S., Kakutani, N., Nambu, H., Yamanashi, K., Furihata, T., Yokota, T., Okita, K., Kinugawa, S., Anzai, T., 2018. Protein acetylation in skeletal muscle mitochondria is involved in impaired fatty acid oxidation and exercise intolerance in heart failure. J. Cachexia Sarcopenia Muscle 9, 844–859.
Vallon, V., Gerasimova, M., Rose, M.A., Masuda, T., Satriano, J., Mayoux, E., Koepsell, H., Thomson, S.C., Rieg, T., 2014. SGLT2 inhibitor empagliflozin reduces renal growth and albuminuria in proportion to hyperglycemia and prevents glomerular hyperfiltration in diabetic Akita mice. Am. J. Physiol. Renal. Physiol. 306, F194–F204.
Wojtczak, L., Schonfeld, P., 1993. Effect of fatty acids on energy coupling processes in mitochondria. Biochim. Biophys. Acta 1183, 41–57.
Xu, L., Nagata, N., Nagashimada, M., Zhuge, F., Ni, Y., Chen, G., Mayoux, E., Kaneko, S., Ota, T., 2017. SGLT2 inhibition by empagliflozin promotes fat utilization and browning and attenuates inflammation and insulin resistance by polarizing M2 macrophages in diet-induced obese mice. EBioMedicine 20, 137–149.
Yokono, M., Takasu, T., Hayashizaki, Y., Mitsuoka, K., Kihara, R., Muramatsu, Y., Miyoshi, S., Tahara, A., Kurosaki, E., Li, Q., Tomiyama, H., Sasamata, M., Shibasaki, M., Uchiyama, Y., 2014. SGLT2 selective inhibitor ipragliflozin reduces body fat mass by increasing fatty acid oxidation in high-fat diet-induced obese rats. Eur. J. Pharmacol. 727, 66–74.
Zinman, B., Wanner, C., Lachin, J.M., Fitchett, D., Bluhmki, E., Hantel, S., Mattheus, M., Devins, T., Johansen, O.E., Woerle, H.J., Broedl, U.C., Inzucchi, S.E., Investigators, E.-R.O., 2015. Empagliflozin, cardiovascular outcomes, and mortality in type 2 diabetes. N. Engl. J. Med. 373, 2117–2128.